MXene-infused bioelectronic interfaces for multiscale electrophysiology and stimulation

Authors: Nicolette Driscoll[1,2,3], Brian Erickson[4], Brendan B. Murphy[1,2,3], Andrew G. Richardson[2,5], Gregory Robbins[6], Nicholas V. Apollo[1,2,3], Georgios Mentzelopoulos[1,2,3], Tyler Mathis[7,8], Kanit Hantanasirisakul[7,8], Puneet Bagga[9,10], Sarah E. Gullbrand[11,12], Matthew Sergison[3,5], Ravinder Reddy[9], John A. Wolf[3,5], H. Isaac Chen[3,5], Timothy H. Lucas[2,5], Timothy Dillingham[6], Kathryn A. Davis[2,13], Yury Gogotsi[7,8], John D. Medaglia[4,13,14], and Flavia Vitale[1,2,3,6,13] *

Affiliations:
[1]Department of Bioengineering, University of Pennsylvania, Philadelphia, PA, USA
[2]Center for Neuroengineering and Therapeutics, University of Pennsylvania, Philadelphia, PA, USA
[3]Center for Neurotrauma, Neurodegeneration, and Restoration, Corporal Michael J. Crescenz Veterans Affairs Medical Center, Philadelphia, PA, USA
[4]Department of Psychology, Drexel University, Philadelphia, PA, USA
[5]Department of Neurosurgery, University of Pennsylvania, Philadelphia, PA, USA
[6]Department of Physical Medicine and Rehabilitation, University of Pennsylvania, PA, USA
[7]Department of Materials Science and Engineering, Drexel University, Philadelphia, PA, USA
[8]A.J. Drexel Nanomaterials Institute, Drexel University, Philadelphia, PA, USA
[9]Department of Radiology, Center for Magnetic Resonance and Optical Imaging, University of Pennsylvania, Philadelphia, PA, USA
[10]Diagnostic Imaging, St Jude Children's Research Hospital, Memphis, TN, USA
[11]Translational Musculoskeletal Research Center, Corporal Michael J. Crescenz VA Medical Center, Philadelphia, PA, USA
[12]McKay Orthopaedic Research Laboratory, Department of Orthopaedic Surgery, University of Pennsylvania, Philadelphia, PA, USA
[13]Department of Neurology, University of Pennsylvania, Philadelphia, PA, USA
[14]Department of Neurology, Drexel University, Philadelphia, PA, USA

*Corresponding author: Email: vitalef@pennmedicine.upenn.edu

Supplementary Materials

Materials and Methods

Figs. S1 to S16

Tables S1 and S2

Legends for movies S1 to S3

Legend for data file S1

Materials and Methods:

Synthesis of Ti_3C_2 MXene

Ti_3C_2 MXene was provided by Murata Manufacturing Co., Ltd. It was produced using the MILD synthesis method *(50)* to create an ink of 30 mg/mL Ti_3C_2 in deionized water, which was placed in a vial and sealed under Argon atmosphere for long term storage.

Fabrication of MXtrode devices

Devices were fabricated by laser-patterning nonwoven textile substrates comprised of hydroentangled 60% cellulose / 40% polyester blend (Texwipe TexVantage) using a CO_2 laser (Universal Laser Systems PLS 4.75) such that electrode array patterns were easily separable from the surrounding textile (7% power, 48% speed), but could still be lifted and handled as one sheet. These were transferred to a thin and slightly tacky bottom layer of 1:10 PDMS (Sylgard 184) on a flat acrylic sheet, and the excess textile surrounding the array patterns was then peeled up. The textile patterns were inked with 20 mg/mL Ti_3C_2 MXene, allowed to air dry for 15 min, then placed in a vacuum oven (Across International) at 70 °C and 60 mmHg for 1 h to remove all remaining water. For devices incorporating 3D mini-pillar electrodes, 3 mm circles were cut from absorbent cellulose sponges (EyeTec Cellulose Eye Spears) using a 3 mm biopsy punch and these circular sponges were inked with MXene and placed onto the electrode locations of the array during the inking step. The subsequent drying steps were identical. For multichannel arrays, connectors (FCI/Amphenol FFC&FPC clincher connectors) were attached by screen printing silver conductive epoxy (CircuitWorks CW2400) onto the ends of the dried MXene constructs, inserting these into the connectors, and clinching shut. The devices were baked at 70 °C for 30 min to cure the silver epoxy. Next, 1:10 PDMS was deposited over the devices to form the top insulation layer, thoroughly degassed at 60 mmHg for 15 min – which forced PDMS to infiltrate into the MXene composite matrix – and subsequently cured at 70 °C for 1 h. Finally, devices were cut out with a razor blade, and peeled up from the acrylic substrate. For planar electrodes, electrode contacts were exposed by cutting circular holes though the top PDMS layer using a biopsy punch (diameters ranging from 500 μm to 3 mm) and carefully peeling up the disk of PDMS to expose the MXene composite electrode below. For 3D mini-pillar electrodes, contacts were exposed by trimming the tops of the mini-pillars with a flat razor blade, exposing the MXene-sponge composite electrode. Slight variations on this method were utilized for MXtrode arrays designed for different applications: for EMG arrays, a thin layer of silicone medical adhesive spray (Hollister Adapt 7730) was applied to the skin-facing side of the array prior to opening the electrode contacts to enhance skin adhesion; for single-channel ECG and EOG MXtrodes, EcoFlex (Smooth-on Ecoflex 00-30) in a 1:2 ratio (part A:part B) was used as the encapsulation rather than PDMS to offer enhanced skin adhesion and comfort; for the ECoG electrodes, arrays were fabricated in PDMS as described above, but were additionally coated in a 1 μm-thick layer of Parylene-C prior to opening electrode contacts to enhance the moisture barrier properties of the encapsulation.

Imaging of MXtrode devices

Optical images of MXtrodes and their constituent parts were taken with a Keyence VHX6000 digital microscope. Scanning electron microscopy (SEM) images were captured using a Zeiss Supra 50VP scanning electron microscope with an accelerating voltage of 5 kV.

Evaluation of textile substrates

The following textile substrates were evaluated as candidates for MXtrode devices: 55% cellulose / 45% polyester nonwoven hydroentangled blend (TechniCloth, Texwipe), 60% cellulose (cell) / 40% polyester (poly) nonwoven hydroentangled blend (TexVantage, Texwipe), 100% cotton nonwoven hydroentangled (G7, FG Clean Wipes), 100% polyester nonwoven (C3, FG Clean Wipes). To evaluate the effect of substrate material on the conductivity of MXene composites, 3 mm x 5 cm laser-cut strips of each material were inked with 60 µL of Ti_3C_2 MXene at 20 mg/mL (1.2 mg total mass of MXene). Samples were allowed to air dry for 1 hr, then were placed in a vacuum oven (Across International) at 70 °C and 60 mmHg for 1 h to remove all remaining water. N=6 samples for each type were probed with a DC multimeter (Fluke) using flat alligator clips to measure end-to-end resistance. Thickness measurements for each textile material were made using digital calipers (Marathon) and averaged over 20 measurements. Conductivity was then calculated as

$$\sigma = \frac{L}{R \cdot A} \tag{1}$$

where L = length of sample, A = cross-sectional area, and R = resistance.

Mechanical testing

The durability of the MXene conductive composites formed with different textile substrates was evaluated by preparing 3 mm x 10 cm laser-cut strips of each substrate, infusing with MXene ink and drying as previously described. Samples were placed in an Instron testing system (Instron 5948) and subjected to 1000 cycles of compression to induce bending, with maximum compression corresponding to a bending radius of 2.5 mm. Throughout the compression testing, resistance was recorded with a sampling rate of 1 Hz using a Gamry Reference 600 potentiostat (Gamry Instruments) *via* alligator clips fixed to each end of the sample. To evaluate the durability of the connection between 3D mini-pillars to the underlying flat substrate in 3D MXtrodes, devices were fixed onto glass slides with epoxy, then plastic rods were epoxied onto the tips of 3 mm-diameter MXtrode mini-pillars in two configurations: one for applying lateral tension, and one for applying vertical tension (pulling the pillar vertically away from the underlying substrate). Force-displacement curves were obtained using the Instron testing system (Instron 5948) until failure.

Optimization of MXene ink concentration

To evaluate the effect of MXene ink concentration on the conductivity of resulting MXene composites, 3 mm x 5 cm laser-cut strips of 60/40 cell/poly were inked with 60 µL of MXene ink at each of the following concentrations: 26, 20, 10, 5, 2, 1, 0.5, 0.05 mg/mL. After thorough drying, end-to-end DC resistance of N=4 samples of each type was measured using a DC multimeter

(Fluke). The 0.05 mg/mL MXene ink sample showed infinite resistance, indicating this concentration was too low to form a continuous conductive network in the composite. The conductivity for each sample was then calculated according to Equation 1.

X-ray diffraction (XRD) imaging

XRD was conducted on pristine textile (TexVantage, Texwipe) and MXene-infiltrated textile to confirm presence of Ti_3C_2 MXene. A Rigaku MiniFlex benchtop X-ray diffractometer (Rigaku Co. Ltd.) with Cu Kα (λ=0.1542 nm) source was used for measurements and the spectra were acquired at 40 kV voltage and 15 mA current for 2Θ values from 3° to 40° at a rate of 7°/min with a step of 0.02°.

Raman spectroscopy

Raman spectra were measured on pristine textile (TexVantage, Texwipe) and MXene-infiltrated textile to confirm presence of Ti_3C_2 MXene. An InVia confocal Raman microscope (Renishaw plc) was used with λ=785 nm, 5% power (~0.15 mW), and a 20x objective. Spectra were measured with 600 lines/mm grating, with 30 s exposure, and averaged across N=4 scans for each sample.

DC conductivity of ink-infused composites

DC conductivity measurements were made on laser-cut test structures 20 cm long x 3 mm wide x 285 μm thick comprising 55% cellulose / 45% polyester blend (Texwipe TechniCloth) infused with either: (1) 20 mg/mL Ti_3C_2 MXene in deionized water, (2) 1.1% high conductivity grade PEDOT:PSS in H_2O (Sigma Aldrich), or (3) 18 mg/mL highly concentrated single-layer graphene oxide (Graphene Supermarket) which was subsequently reduced using a vitamin C reduction method *(88)*. Measurements were taken with a handheld multimeter with flat alligator clip terminations, where the negative lead was fixed at the end of the construct and the positive lead was moved in 2 cm increments for each measurement.

Electrochemical characterization

For cutaneous EIS measurements, the skin of the inner forearm was prepared with an alcohol swab followed by light abrasion (3M TracePrep abrasive tape) before placing 3 mm planar and 3D mini-pillar MXtrodes and measuring EIS from 1 to 10^5 Hz with a 10 mV_{pp} driving voltage using a Gamry Reference 600 potentiostat. Reference was placed on the inner wrist and ground was placed on the elbow (Natus disposable disk electrodes). Electrochemical measurements in saline, including EIS, CV, and current pulsing, were performed for planar MXtrodes with diameters of 3 mm, 2 mm, 1 mm, and 500 μm, and Pt electrodes with a diameter of 2 mm in 10 mM phosphate buffered saline (Quality Biological, pH 7.4) using a Gamry Reference 600 potentiostat. Pt electrodes were fabricated by sputtering 10 nm Ti followed by 100 nm Pt (Denton Explorer-14 magnetron sputter system) on Kapton films and subsequently encapsuling these films in Kapton tape with a 2-mm opening pre-cut to form the electrode. All electrochemical measurements were done in a 3-electrode configuration with a graphite rod counter electrode (Bio-Rad Laboratories, Inc.) and an Ag/AgCl reference electrode (Sigma-Aldrich). EIS was measured from 1 to 10^5 Hz with 10 mV_{pp} driving voltage. Cyclic voltammetry was performed at a sweep rate of 50 mV/s. Water window voltage limits for MXtrodes were determined by incrementally increasing the

negative limit of the CV scan until water reduction was observed (beginning at −1.9 V), then the positive limit of the CV scan until a linear, resistive behavior was observed (beginning at +0.7 V) beyond which the MXtrode showed current loss with subsequent scans. Stability in the MXene water window (−1.7 to +0.6 V) was evaluated by CV cycling 500 µm MXtrodes 50 times in this window at 50 mV/s. CSC_c was determined from CV scans by taking the time integral of the cathodic current. Current pulsing was performed using chronopotentiometry with biphasic, charge-balanced current pulses with $t_c = t_a = 500$ µs and $t_{ip} = 250$ µs for currents ranging from 600 µA to 5 mA for N=5 electrodes of each size. For CIC_c calculations, E_{mc} was determined as the instantaneous voltage 10 µs after the end of the cathodic current pulse. E_{mc} values were plotted as a function of injected current amplitude, and the linear relation was determined to estimate the current limit at which the electrode would reach its cathodic limit (−1.7 V for MXtrodes, −0.6 V for Pt). Any series of measurements in which current amplitude vs. E_{mc} was not linear with $R^2 < 0.95$ were excluded. CIC_c was defined as:

$$CIC = \frac{I_{lim} \times t_c}{GSA}, \quad (1)$$

where I_{lim} is the cathodic current limit, t_c is the cathodic pulse width, and GSA is the electrode geometric surface area. CSC and CIC scaling relations were determined by fitting power functions to the data, similar to work by M. Ganji *et al*. *(61)*.

EEG experiments

EEG experiments were conducted under a protocol approved by the IRB of Drexel University (Protocol # 1904007140). One healthy human subject was seated in a comfortable chair and the recording area on subject's scalp was prepared with an alcohol swab and light abrasion (3M TracePrep abrasive tape), though the presence of hair may have limited the efficacy of the skin abrasion. Recordings were made using an 8-ch MXtrode array consisting of 3 mm-diameter 3D mini-pillar electrodes arranged in a 25 mm diameter circular ring (9.5 mm inter-electrode spacing) and one standard 10 mm-diameter gelled Ag/AgCl EEG cup electrode (Technomed Disposable EEG cup) placed in the center of the MXtrode array. The Ag/AgCl EEG electrode was filled with conductive gel (SuperVisc, EASYCAP GmbH) and all electrodes were held in place using pre-wrap (Mueller). Recordings were obtained using a NeuroNexus SmartBox amplifier system with a sampling rate of 20 kHz. Standard gelled Ag/AgCl EEG cup electrodes were used for reference (placed on left mastoid) and ground (placed on forehead center). In the first set of recordings, electrodes were positioned on the parietal region, centered over 10-20 site P1. To evoke identifiable changes in the alpha band *(1)(89)*, six 2-minute-long recordings were obtained, alternating between eyes open and eyes closed states. During resting state, the subject was instructed to remain relaxed but alert. For the eyes open state, the subject was asked to fixate on a cross on a computer monitor to reduce oculomotor saccades and maintain a consistent degree of external vigilance. In the second set of EEG recordings, the hand motor region was localized using single TMS pulses to isolate a location that evoked lateral finger movements *(90)*, and the electrodes were centered over this location, approximately at site C3. Six 2-minute-long recordings were obtained, cycling through a resting state, imagined hand flexion, and actual hand flexion. Signals were notch filtered at 60 Hz and bandpass filtered from 0.1 – 100 Hz. Bridging analysis was performed to ensure that gel did not leak from the Ag/AgCl electrode to contact any recording

surface in the MXtrode array. Frontal EEG recording experiments were performed on N=3 additional subjects using a 32-ch bi-frontal montage of MXtrodes. Two 16-ch MXtrode arrays with 3 mm-diameter 3D mini-pillar electrodes and 3 mm inter-electrode spacing arranged in a 4x4 grid were placed over 10-20 EEG locations F3 and F4 after skin preparation. Skin preparation included wiping the skin with an alcohol swab followed by light abrasion (3M TracePrep abrasive tape). Reference and ground electrodes were 20 mm-diameter pre-gelled electrodes (Natus disposable adhesive electrodes) placed on the left and right mastoids. Recordings were obtained using an Intan RHS amplifier (Intan Technologies) at a 20 kHz sampling rate. Subjects alternated between eyes open and eyes closed states for 2 mins each. During resting state, the subject was instructed to remain relaxed but alert. For the eyes open state, the subject was asked to fixate on a cross on a computer monitor to reduce oculomotor saccades and maintain a consistent degree of external vigilance.

EMG and ECG experiments

EMG and ECG epidermal recordings were conducted under a protocol approved by the IRB of the University of Pennsylvania (Protocol # 831802). For all epidermal experiments, skin preparation prior to placing MXtrode arrays included an alcohol swab followed by light abrasion (3M TracePrep abrasive tape), and signals were recorded at a sampling rate of 20 kHz on an Intan RHS2000 Stimulation/Recording Controller (Intan Technologies). Recordings from abductor pollicis brevis (APB) at the base of the thumb were obtained using a 5x4 grid of 3 mm planar MXtrodes with center-to-center spacing of 7.5 mm horizontal, 6.5 mm vertical. Reference was placed over the bony interphalangeal thumb joint and ground was placed on the back of the hand (Natus disposable adhesive electrodes). The median nerve was stimulated at the wrist using a VikingQuest handheld bipolar stimulator (Nicolet), starting at 10 mA and gradually increasing until supramaximal activation of the APB was achieved in the form of a thumb twitch (amplitude 38.8 mA for the subject shown). For localization of the NMJ of the APB, evoked responses recorded on each electrode in the array (no signal filtering was used) were averaged across all stim trials (N=10), the peak of the average evoked response was determined, and a map of the latency of this peak from the onset of the stimulation was created. The location of the NMJ was approximated as the location with the shortest latency in the peak evoked response. For recordings of the biceps, a 10x4 grid of 3 mm planar MXtrodes with center-to-center spacing of 8.5 mm horizontal, 8.5 mm vertical, was placed over the center of the biceps muscle. Reference was placed distal to the array just above the inner elbow and ground was placed proximal to the array on the deltoid (Natus disposable adhesive electrodes). The supraclavicular nerve was stimulated using the same VikingQuest handheld bipolar stimulator (Nicolet), starting at 30 mA and gradually increasing until clear submaximal activation of biceps was observed (amplitude 49.0 mA for the subject shown). As for the APB recordings, evoked responses recorded on each electrode were averaged across all stim trials (N=11), the peak of the average evoked response was determined, and a map of the latency of this peak from the onset of the stimulation was created. The IZ was determined as the area with the shortest latency in the peak evoked response. To further validate the IZ localization in the biceps, additional EMG recordings were made with the subject performing periods of isometric voluntary contractions. Signals were subtracted in bipolar configuration down the length of the MXtrode array, and MUAPs were identified in the raw EMG

signal. The IZ was determined as the region where the MUAP appears earliest and where the signal polarity inverts.

Motion and pressure artifacts evaluation

To evaluate motion artifacts, an array of 3 mm-diameter planar MXtrodes was placed directly adjacent to a 20 mm-diameter pre-gelled electrode (Natus disposable disk electrodes) on the inner forearm of a healthy human subject following skin preparation including cleaning with an alcohol swab and light abrasion (3M Trace Prep tape). Reference and ground were 20 mm-diameter pre-gelled electrodes (Natus disposable disk electrodes), placed on the elbow and inner wrist, respectively. A load cell (Omega Engineering, Inc.) was grasped between the thumb and forefinger to record the force during a pinching grip. Recordings were obtained using an Intan RHS amplifier (Intan Technologies) at 20 kHz. The subject alternated between 2 min periods of (1) periodic pinching of the load cell to produce EMG and (2) a relaxed grip while vigorously moving the arm up and down, hinging at the elbow. For the arm motions, the opposite hand was used to lift the arm to avoid activating the forearm muscles during this motion and isolate motion artifacts from true EMG signal. To evaluate pressure artifacts, the load cell was then used to apply periodic force directly down onto the electrodes, while recording in the same configuration. A flat piece of plastic was used to distribute the force across all MXtrodes as evenly as possible. The load cell force limit is 2 kg, at which point the signal saturates. During this evaluation some of the applied forces exceeded 2 kg.

ECG recording

For ECG recording experiments, skin preparation prior to placing electrodes included an alcohol swab followed by light abrasion (3M TracePrep abrasive tape), and signals were recorded at a 20 kHz sampling rate on an Intan RHS2000 Stimulation/Recording Controller (Intan Technologies). Recordings were made in a 3-electrode configuration with reference placed just below the subject's right clavicle, ground placed just below the subject's left clavicle, and the working electrode placed on the lower left ribs. For comparison, recordings were made sequentially using either 2 cm gelled Natus electrodes (Natus disposable adhesive electrodes) or 1.3 cm dry MXtrodes, with electrodes placed in the same locations.

EOG recording

EOG recordings were conducted under an experimental protocol approved by the IRB of the University of Pennsylvania (Protocol # 831802). Skin preparation prior to placing the electrodes included an alcohol swab followed by light abrasion (3M TracePrep abrasive tape), and signals were recorded at a 20 kHz sampling rate on an Intan RHS2000 Stimulation/Recording Controller (Intan Technologies). 1.3 cm-diameter dry MXtrodes were used for ground, (+) and (-) contacts. For tracking up-down eye movements, the (+) and (-) electrodes were placed below and above the right eye, respectively. The subject moved their eyes in a center-down-center-up-center pattern for 2 minutes. For tracking left-right eye movements, the (+) and (-) electrodes were placed just lateral to the left and right eyes, respectively. The subject moved their eyes in a center-left-center-right-center pattern for 2 minutes. The ground electrode was centered on the forehead for both EOG recording paradigms.

ECoG recording

ECoG recording was performed in N=1 pig. All experiments were conducted according to the ethical guidelines set by the Institutional Animal Care and Use Committee of the University of Pennsylvania and adhered to the guidelines set forth in the NIH Public Health Service Policy on Humane Care and Use of Laboratory Animals (2015). Pigs were pair housed when possible and were always in a shared room with other pigs in a research facility certified by the Association for Assessment and Accreditation of Laboratory Animal Care International (AAALAC facility). Prior to the procedure, the animal was fasted for 16 hours with water remaining ad libitum. After induction with 20 mg/kg of ketamine (Hospira, 0409-2051-05) and 0.5 mg/kg of midazolam (Hospira, 0409–2596-05), anesthesia was provided with using 2−2.5% isoflurane (Piramal, 66794-013-25) via a snout mask and glycopyrrolate was given subcutaneously to curb secretions (0.01 mg/kg; West-Ward Pharmaceutical Corp., 0143-9682-25). The animal was intubated with a size 6.0 mm endotracheal tube and anesthesia was maintained with 2−2.5% isoflurane per 2 liters O_2. The animal was then moved to an operating room, and transferred onto a ventilator. The ventilator provided the same rate of isoflurane and O_2 for anesthesia maintenance at a rate of 20-25 breaths per minute. Heart rate, respiratory rate, arterial oxygen saturation, end tidal CO_2, blood pressure and rectal temperature were continuously monitored, while pain response to pinch was periodically assessed. These measures were used to maintain adequate anesthesia. A forced air warming system was used to maintain normothermia. Prior to electrode insertion, the pig was placed in a stereotaxic frame described previously *(91)*, and the surgical site was prepared and draped in the standard sterile fashion. After the skull was exposed, an 11 mm craniectomy was performed at the recording site, 7 mm lateral to midline and 4.5 mm posterior to bregma to expose the frontoparietal cortex. The dura was opened to expose the cortical surface and the MXtrode array was then placed in the subdural space for recording. Recordings were obtained using an HS-36 amplifier and collected continuously at 32 kHz using a Neuralynx Digital Lynx SX recording system. Raw data was collected and stored using Neuralynx's Cheetah recording software. Following the recording, the pig was euthanized and brain tissue was extracted for histology for a separate study.

Cortical stimulation

An adult male Sprague Dawley rat (Crl:SD, 300 g) was used for the stimulation experiment. Anesthesia was induced with 5% isoflurane and the rat was placed in a stereotaxic frame. Depth of anesthesia was monitored by respiratory rate and pedal reflex and maintained at a surgical plane with 1.5−2.5% isoflurane. Whisker motor cortex (wM1) was exposed bilaterally with a craniotomy centered on the midline. A durotomy was performed over right wM1. A stimulation return skull screw was placed in the left frontal bone. Trains of biphasic current pulses (300 µs/phase, 3 µs interpulse interval, 100 pulses, variable pulse amplitude from 1.0 to 1.4 mA) were delivered through a single electrode in the MXtrode array using the Intan RHS System (Intan Technologies). Stimulus-evoked contralateral whisker movement was quantified with a laser micrometer (IG-028, Keyence Corp.), which had a measurement range of 28 mm, a spatial resolution of 5 µm, and a temporal resolution of 490 µs. A 360 µm diameter polyimide tube was placed over a whisker with visually apparent stimulus evoked movement. Spatial sensitivity of the micrometer was adjusted to detect only the motion of the whisker in the tube *(2)*. At the conclusion of the experiment, the

rat was killed with an intraperitoneal injection of sodium pentobarbital. These procedures were approved by the Institutional Animal Care and Use Committee of the University of Pennsylvania.

Evaluation of MRI and CT compatibility

A strip of six 3 mm-diameter MXtrodes were prepared with PDMS encapsulation to match the geometry of comparison Pt clinical ECoG electrode strips (Adtec epilepsy subdural grid TG48G-SP10X-000). Both types of electrode arrays were placed in 0.6% agarose (IBI Scientific) prepared with 10 mM PBS (Quality Biological, pH 7.4) in a 15 mm inner-diameter glass test tube, with degassing to remove air bubbles. A 9.4 T Horizontal bore MRI scanner (Bruker, Erlangen) and 35 mm diameter volume coil (m2m Imaging, USA) were used to acquire T1-weighted gradient echo MR images of cross-sections of both electrode types. The acquisition parameters for T1-Wighted MRI were: echo time (TE)/ repetition time (TR) = 7/150 ms, field of view (FOV) = 30x30 mm^2, Matrix size = 256x256, Averages = 4, Flip angle = 30°, slice thickness = 0.7 mm. For CT imaging, a μCT50 specimen scanner (Scanco Medical, Bruttisellen, Switzerland) was used to scan the electrodes at 70 kV, 115 μA, and 10 μm isotropic resolution. 2D images in the axial plane of each electrode type were acquired for comparison. Following these evaluations, additional MXtrode devices were imaged in a 3T clinical MRI scanner (Siemens MAGNETOM Prisma). An array of 3 mm-diameter 3D mini-pillar MXtrodes was placed on an FBirn MRI phantom with a vitamin E marker over the 3D electrodes. The device was imaged using T1-weighted MPRAGE, T2-weighted TSE, FLAIR 3D, and HCP resting BOLD sequences. The temperature of the device during scan sequences was continuously monitored using a fiber optic temperature sensor (Neoptix T1) fixed in direct contact with one of the MXtrode mini-pillars and through IR imaging the device at the conclusion of scan sequences. After observing no noticeable artifacts or heating, the device was then placed on the forehead of a healthy human subject and the same scan sequences were repeated. The experimental protocol was approved by the IRB of the University of Pennsylvania (Protocol # 819126) and the participant gave informed consent.

Magnetic susceptibility measurements

Magnetic properties of Ti_3C_2 were measured with Quantum Design EverCool II physical property measurement system. A free-standing film of Ti_3C_2 with a mass of 4.820 mg was packed in a plastic sample container. The sample was heated to 310 K and was allowed to reach thermal equilibrium for about 10 min. Magnetization was recorded with respect to the applied magnetic field up to 9 T. The measured data was subtracted from that of the plastic sample holder and normalized by sample mass.

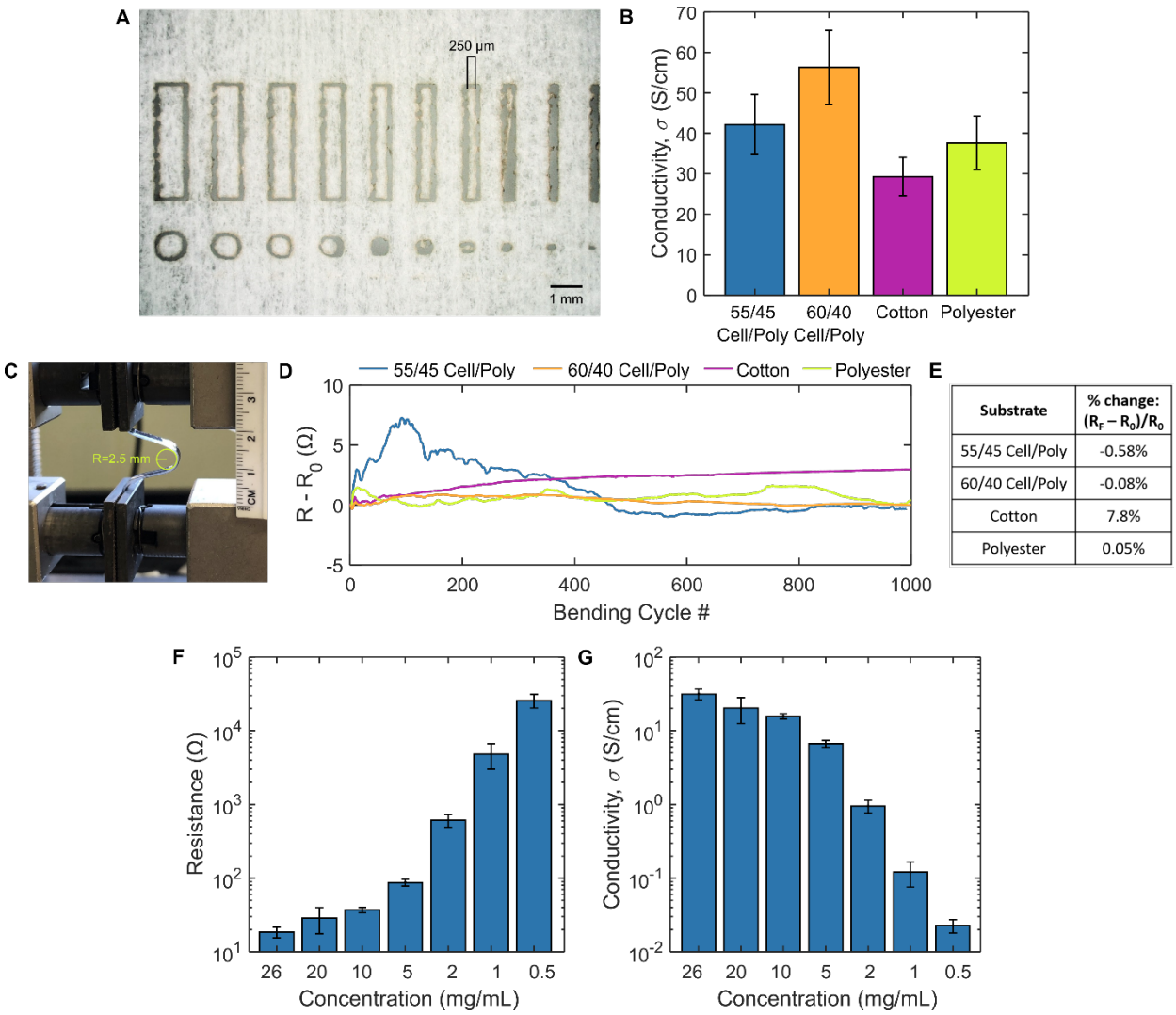

Fig. S1. Fabrication optimization. (**A**) Photograph of incrementally smaller patterns cut with CO_2 laser, showing maximum resolution of ~250 µm. (**B**) Conductivity of composites from different textile substrate materials, each inked with identical amount of MXene (N=6 for each material). 55/45 Cell/Poly and 60/40 Cell/Poly correspond to nonwoven blends of 55%/45% cellulose/polyester and 60%/40% cellulose/polyester. (**C**) Photograph of bend cycling test setup. Composites were subjected to cycling bending to a 2.5 mm radius of curvature for 1000 cycles. (**D**) Change in resistance across 1000 bending cycles. (**E**) Table showing % change in resistance after 1000 bending cycles. The 60/40 Cellulose/Polyester blend was chosen for the fabrication of all the devices used in the rest of the study. (**F**) Resistance and (**G**) conductivity of 3 mm x 5 cm constructs inked with different concentrations of MXene ink (N=4 for each concentration). The high viscosity of the 26 mg/mL ink prevented uniform infiltration into the substrate, instead forming a MXene layer on the surface, thus 20 mg/mL was chosen as the ink concentration for all the subsequent device fabrication.

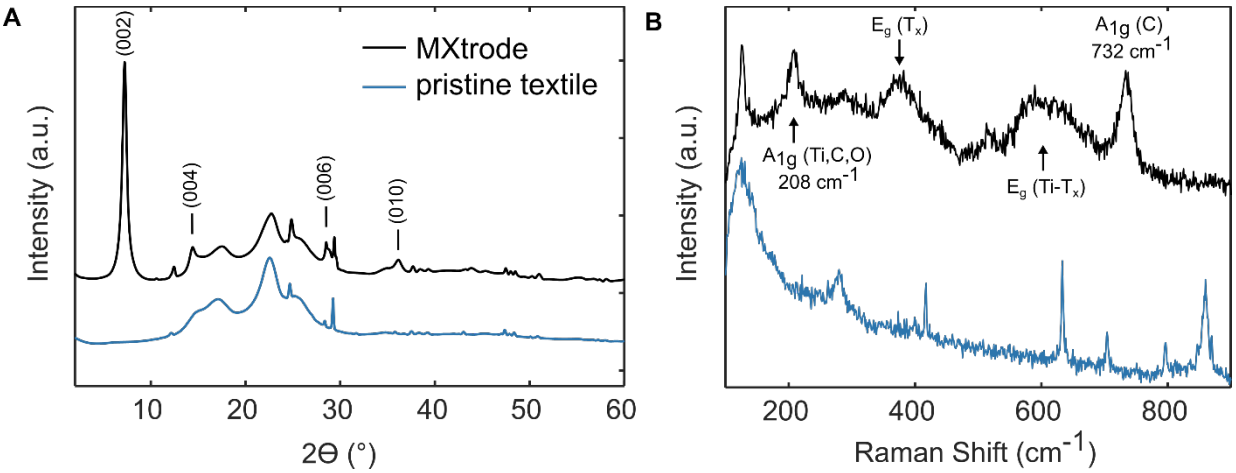

Fig. S2. Diffraction and spectroscopic analysis of MXtrode composite. (**A**) X-ray diffraction (XRD) patterns of pristine textile (cellulose/polyester blend) and Ti_3C_2 MXene-infused textile. The labelled peaks in the MXtrode pattern correspond to the (00*l*) family of planes, defined by the interlayer spacing, where *l*=2,4,6,8,10, *etc*. These reflections correspond to the out-of-plane stacking of single-layer MXene flakes, and they are absent in the spectra for the pristine textile. The textile peak at 2Θ=23.2° corresponds to the (002) reflection of cellulose. (**B**) Raman spectroscopy of the same samples shown in (**A**). The labelled peaks in the MXtrode spectra correspond to known A_{1g} out-of-plane and E_g in-plane Raman peaks for Ti_3C_2 MXene, which are distinguishable from the pristine textile. Here, T_x represents the surface terminations O_2, O(OH), and $(OH)_2$.

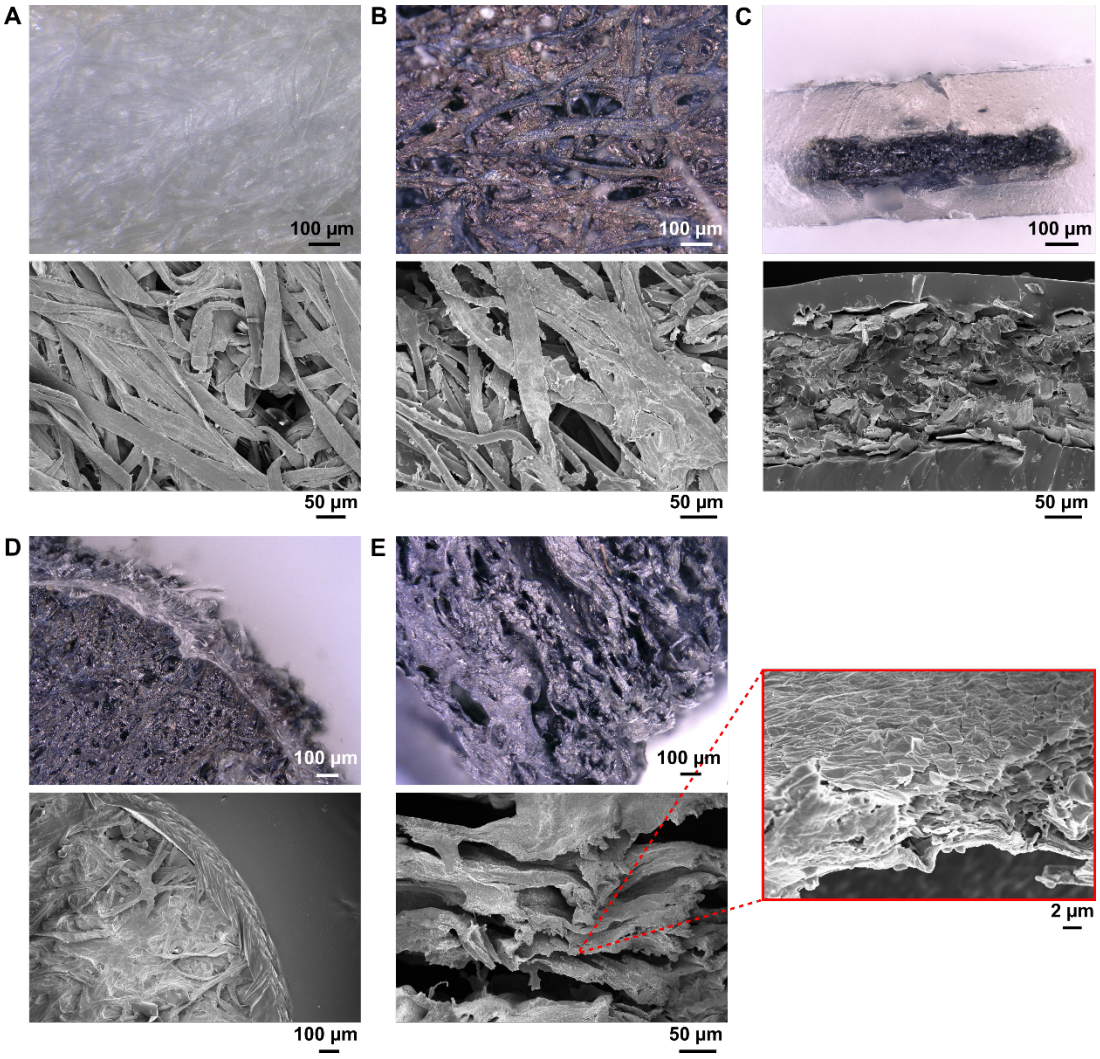

Fig. S3. Optical and SEM images of MXtrode composites. Optical microscopy images (top panel) and corresponding SEM images (bottom panel) for: (**A**) pristine 60/40 cellulose/polyester blend substrate, (**B**) the same substrate after infusing with MXene ink, (**C**) cross-section of MXene composite trace embedded in PDMS, (**D**) edge of planar electrode contact, (**E**) side of MXene-infused cellulose foam in 3D mini-pillar MXtrode.

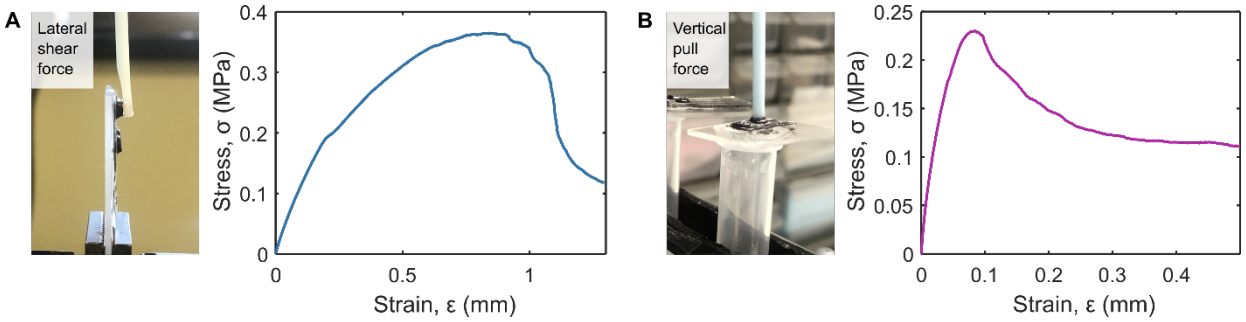

Fig. S4. Durability of 3D pillars. (**A**) Tensile strength testing of the attachment of the 3D pillar to the underlying substrate following encapsulation in PDMS, with force applied in the lateral direction. (**B**) Tensile strength testing similar to (**A**), with the force now directed vertically. Left panels in (A) and (B) show photographs of test setup.

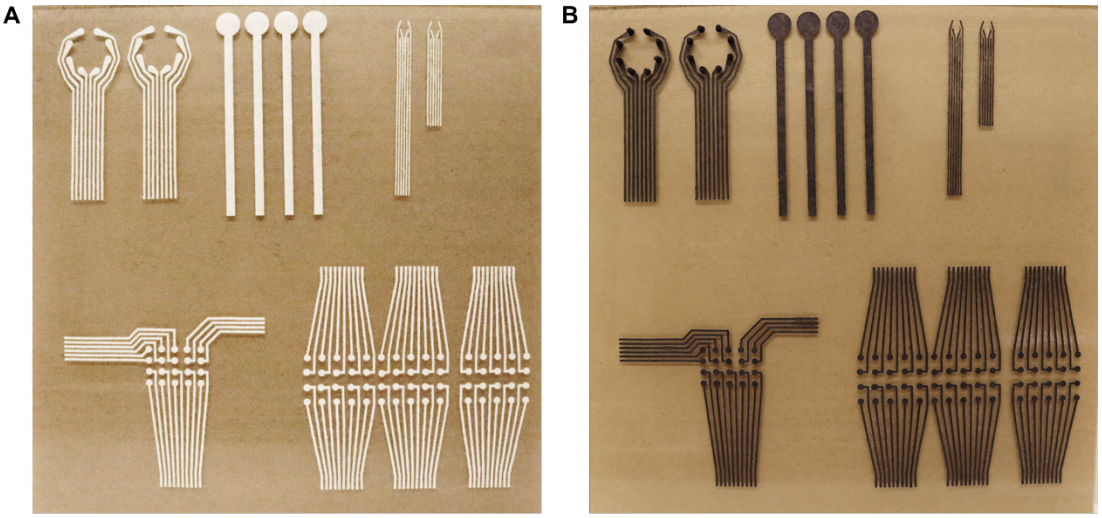

Fig. S5. Scalable fabrication of MXtrode arrays. (**A**) Photo of laser-patterned array substrates for various device and array geometries. (**B**) The same batch of devices shown in (A) after infiltrating with MXene ink. Devices in the top left are EEG ring MXtrode arrays after addition of the 3D mini-pillars.

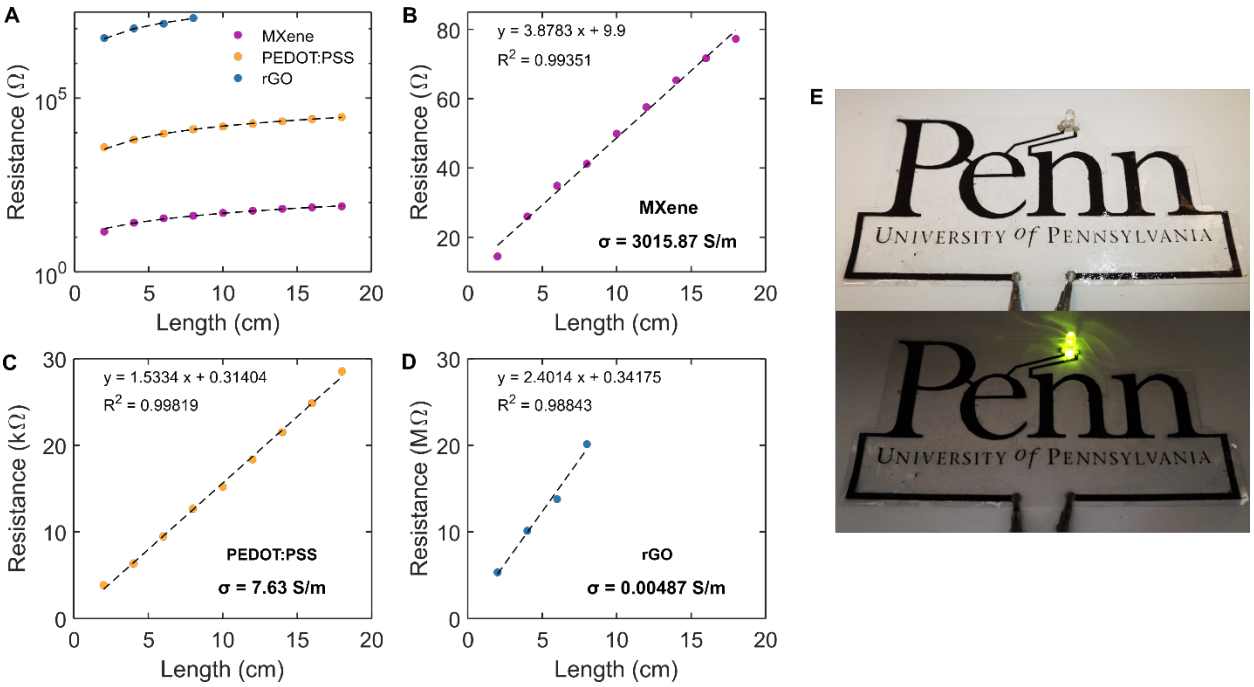

Fig. S6. DC conductivity of ink-infused composites. (**A**) Plot of length vs. DC resistance for composites made using MXene, PEDOT:PSS, and rGO as the conductive ink. Test structures were 20 cm x 3 mm x 285 μm (L x W x H) strips. (**B-D**) Individual plots of DC resistance *vs.* length for (**B**) MXene, (**C**) PEDOT:PSS, and (**D**) rGO, with linear fitting curves shown as dashed lines. The linear relation of resistance *vs.* length, along with the cross-sectional area of the test structure, is used to compute the bulk conductivity, **σ**, of the composites. DC resistance of the rGO composite could only be measured out to 8 cm due to high resistance. (**E**) Photograph of the MXene composite used as conductive trace to power an LED.

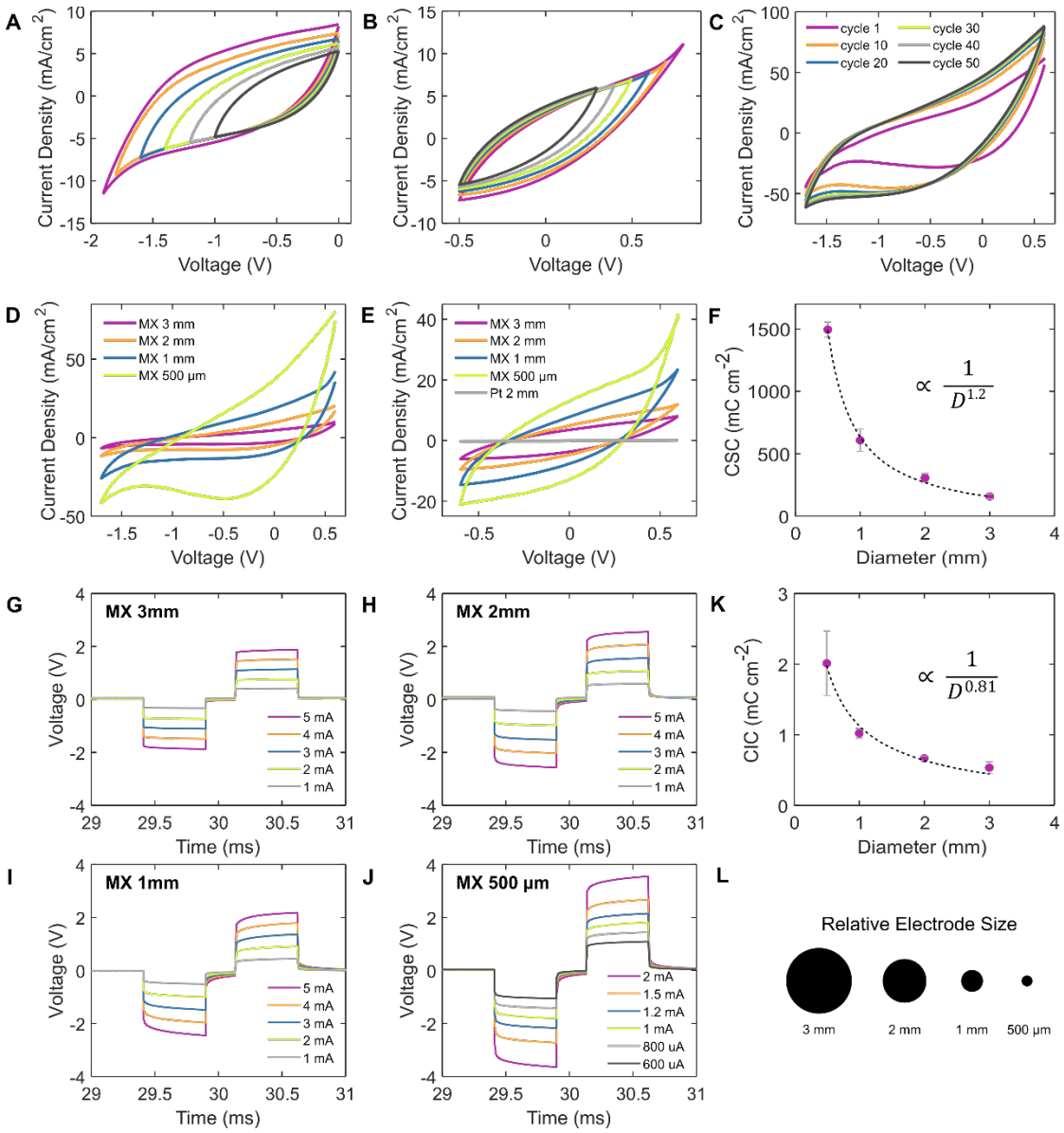

Fig. S7. Scaling of electrochemical properties for MXtrodes. (**A**) CVs probing the negative voltage limit for MXtrodes at 50 mV/s. Hydrolysis of water begins at −1.9 V. (**B**) CVs probing the positive voltage limit for MXtrodes. Current loss and evidence of faradaic current begins at +0.7 V. Test electrode for (A) and (B) was 3 mm-diameter planar MXene. (**C**) Stability of MXtrode within −1.7 V to 0.6 V range as evidenced by cycling a 500 µm MXtrode 50 times at 50 mV/s. (**D**) CVs in MXene safe voltage window, −1.7– +0.6 V, for 3 mm, 2 mm, 1 mm, and 500 µm-diameter MXtrodes. (**E**) CVs in MXene-Pt intersection window, −0.6 to +0.6 V, for 3 mm, 2 mm, 1 mm, and 500 µm-diameter planar MXtrodes and 2 mm-diameter Pt electrode. (**F**) Charge storage capacity of scaled planar MXtrodes as a function of diameter, highlighting the CSC scaling dependence on the electrode diameter. (**G-J**) Voltage transients for biphasic current pulses, with t_c = t_a = 500 µs and t_{ip} = 250 µs, for currents ranging from 1 to 5 mA for (**G**) 3 mm, (**H**) 2 mm, (**I**) 1 mm, and (**J**) 500 µm-diameter planar MXene electrodes. (**K**) Charge injection capacity of scaled planar MXtrodes as a function of diameter, highlighting the CIC scaling dependence on the electrode diameter. (**L**) Schematic demonstrating the relative size of the electrodes used in the study.

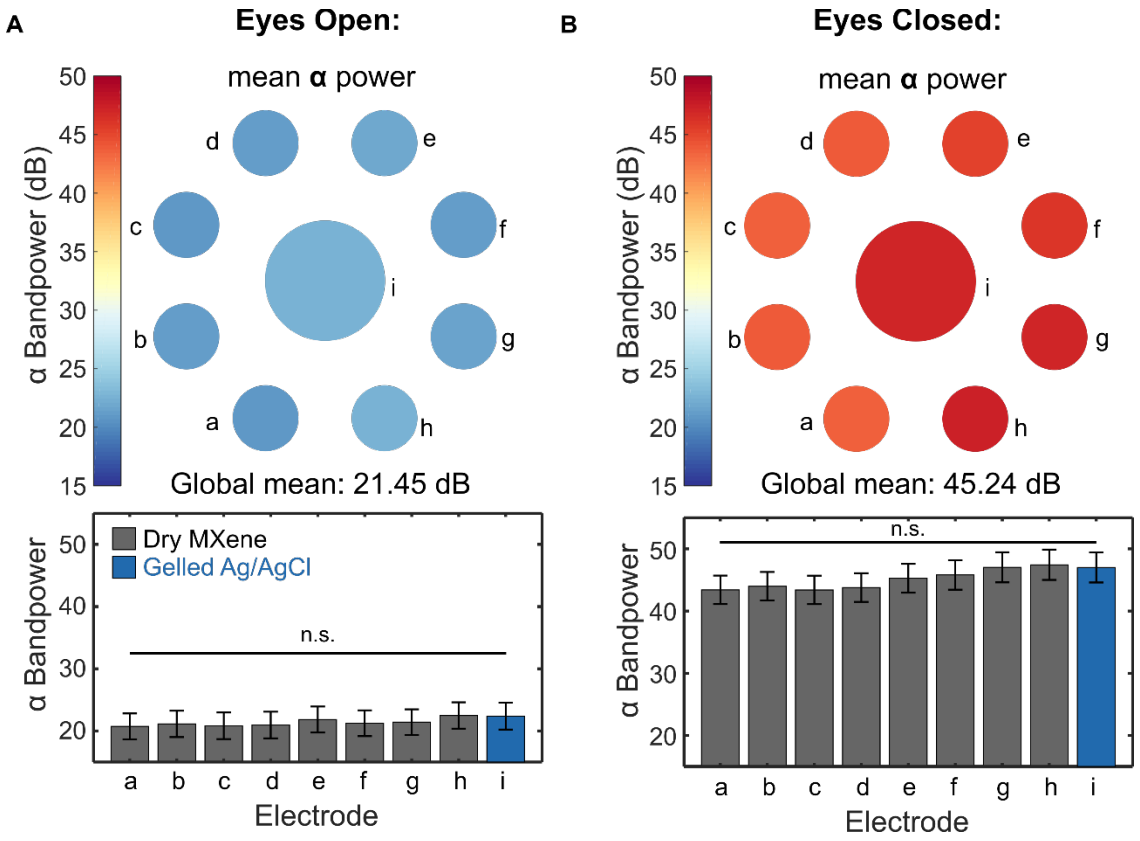

Fig. S8. Parietal EEG alpha bandpower mapping. (**A**) 8-12 Hz alpha bandpower across the 2 min recording in the eyes open state on one human subject. Color plot (top) shows average alpha power for each electrode, mapped to its corresponding location on the scalp. Bar plot (bottom) shows average alpha power, with error bars corresponding to standard error of the mean across all time windows. Statistical significance was calculated using one-way ANOVA. The gelled Ag/AgCl electrode is labelled i and the dry MXtrode electrodes are labelled a-h. (**B**) The same alpha bandpower analysis shown in (A), for the eyes closed task. Statistical significance was calculated using one-way ANOVA. $P > 0.05$, not significant, n.s.

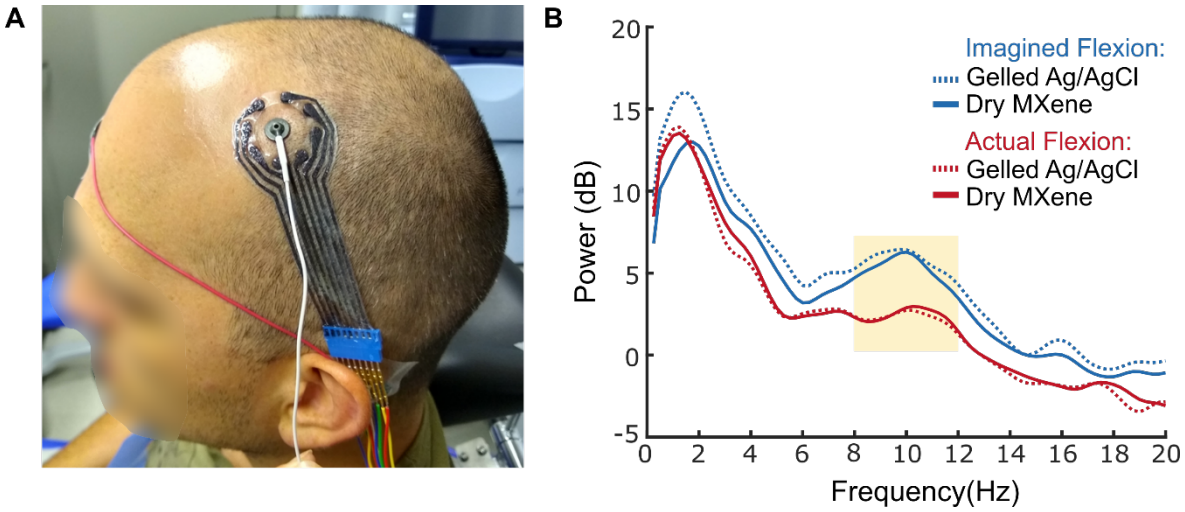

Fig. S9. Motor EEG recording. (**A**) Photograph of the EEG recording setup with electrodes centered over the hand motor region, as localized with single TMS pulses. (**B**) Power spectral densities of the recorded EEG signal reveal a suppression of the 8-12 Hz (shaded) motor mu rhythm during actual hand flexion as compared to imagined hand flexion. N=1 electrode shown for each condition.

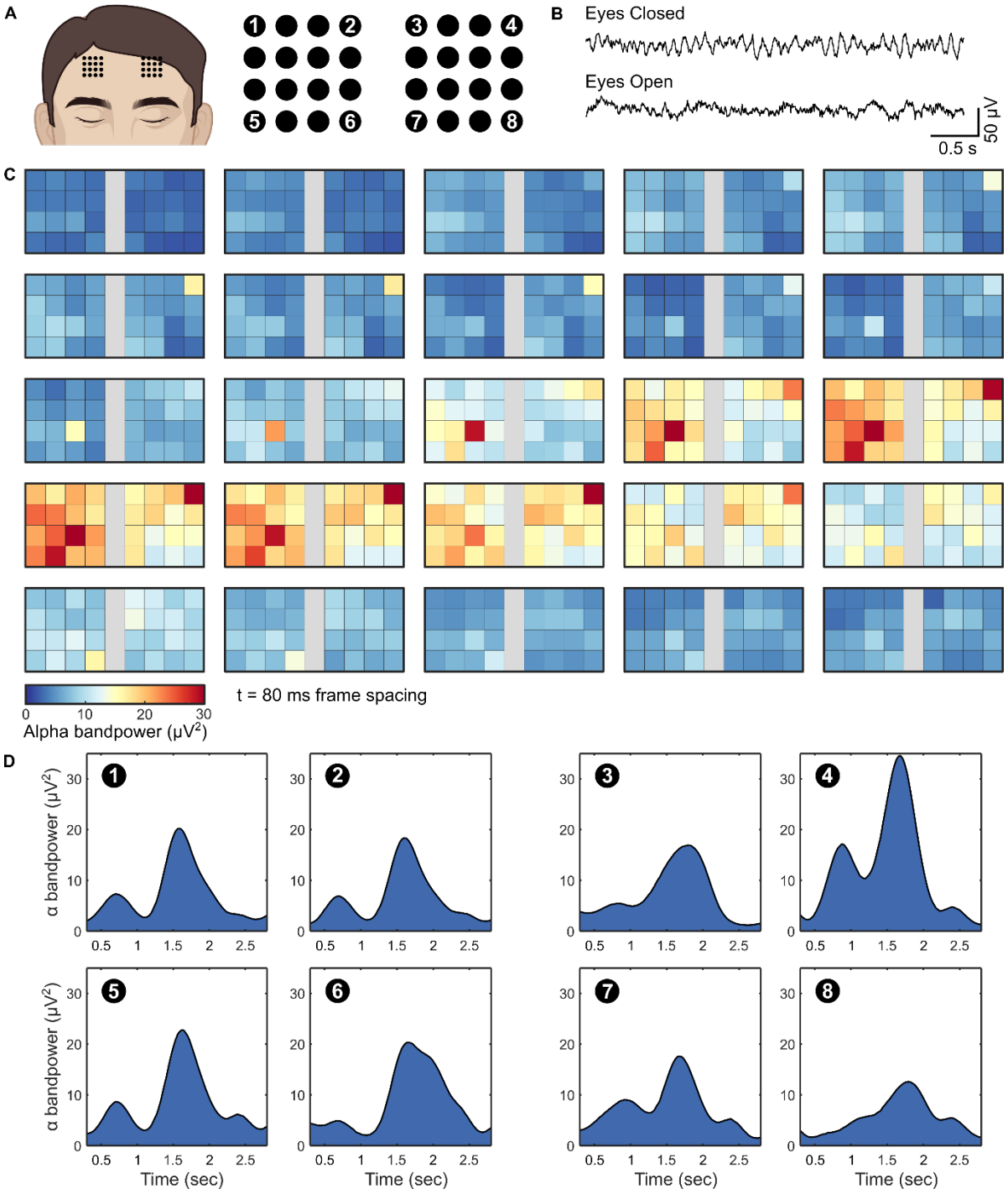

Fig. S10. Bifrontal EEG alpha bandpower mapping. (**A**) Schematic of the EEG recording montage. Two 4x4 grids of 3 mm-diameter MXtrodes with 3 mm inter-electrode spacing were centered over standard 10-20 EEG locations F3 and F4. (**B**) Representative examples of EEG traces from one subject recording during eyes closed and eyes open states, showing clear alpha signature in eyes closed state. (**C**) 8-12 Hz alpha bandpower mapped across the bifrontal montage over time, showing spatial variation in activation. (**D**) Alpha bandpower envelope corresponding to the frames shown in (C) for 8 selected channels, whose locations in the montage are shown in (A).

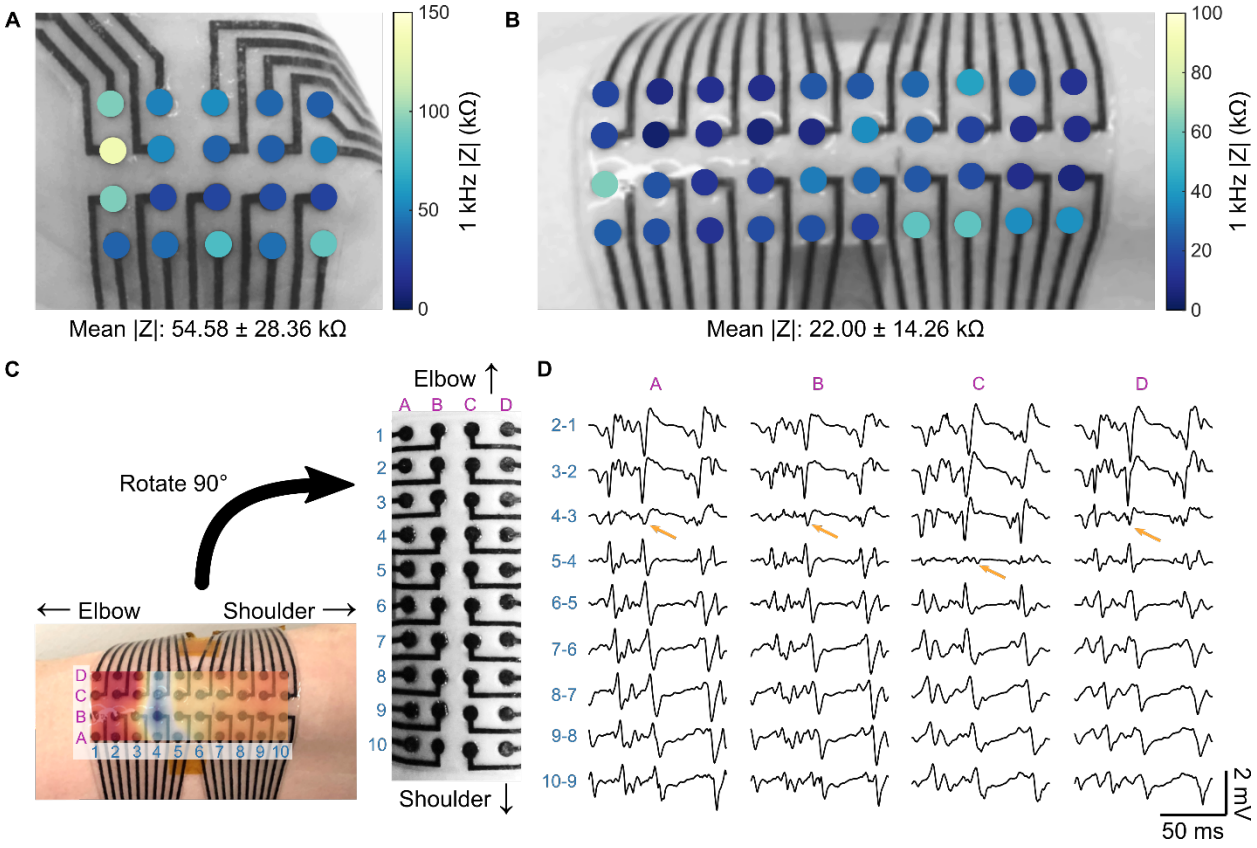

Fig. S11. EMG array impedance and bipolar subtraction experiment. (**A, B**) 1 kHz impedance magnitude maps for the (A) 20-ch planar MXtrode array used to map the *abductor pollicis brevis* muscle and the (B) 40-ch planar MXtrode array used to map the *biceps brachii*, overlaid on images of the arrays on the subject during the experiment. Each muscle recording was performed on N=1 human subject. (**C**) Schematic showing the arrangement for bipolar signal subtraction shown in (**D**) for resisted flexion EMG recordings on the biceps. The latency map obtained from the supraclavicular stimulation experiment is shown overlaid on the bottom image. (**D**) Bipolar EMG signals recorded during resisted flexion on the biceps. The location of the innervation zone is indicated by the arrows, and is clear from the propagation of the EMG signal outward from this region with some delay, as well as the inversion of the spikes on either side. The innervation zone determined from this analysis is in agreement with the region identified by the electrical stimulation-derived latency map shown in (C).

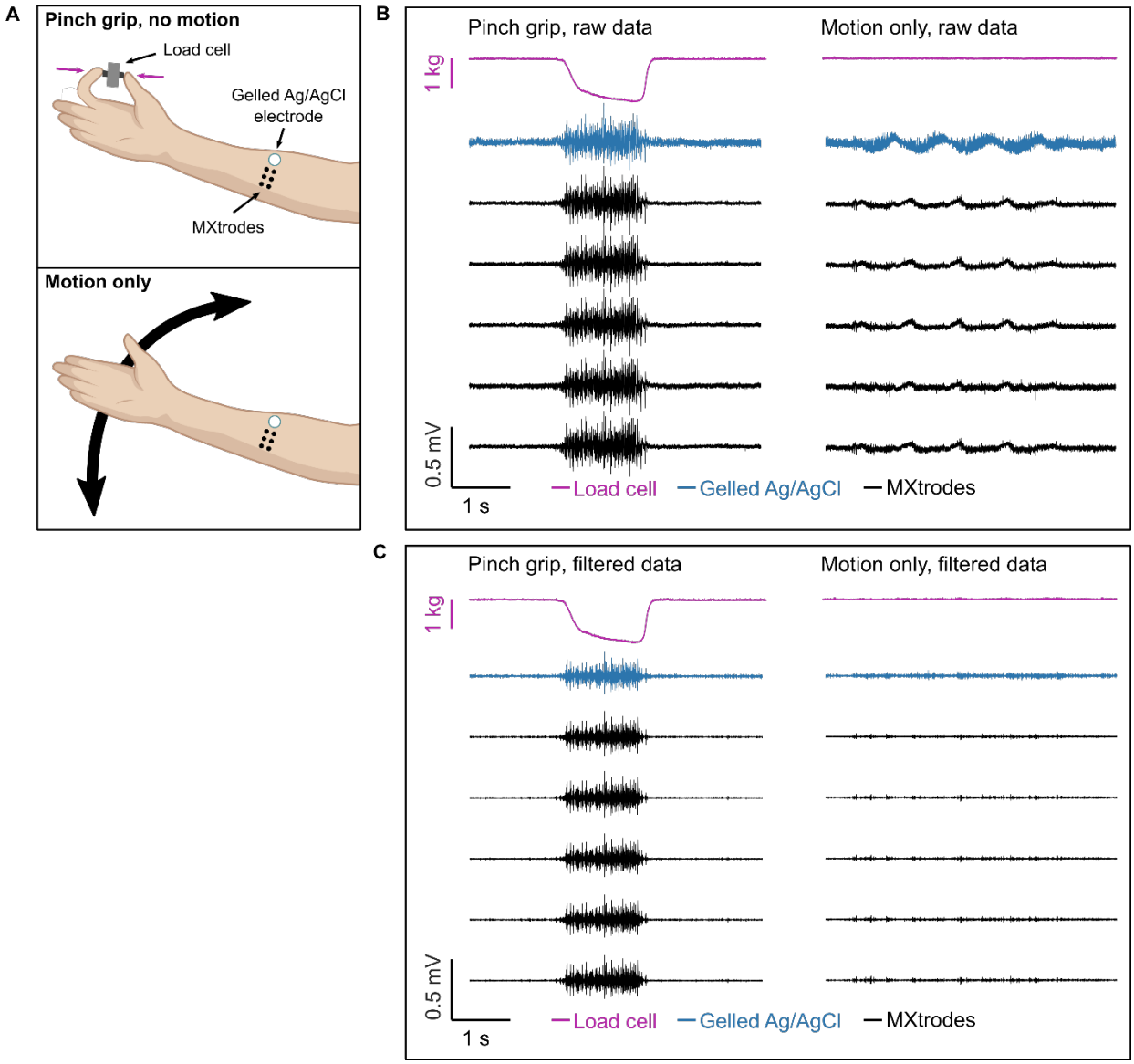

Fig. S12. Motion artifacts evaluation. (**A**) Schematic depicting the two conditions tested: stationary pinch grip, with force recorded using a load cell (top) and up and down motions of the arm (bottom). 3 mm-diameter planar MXtrodes and a 2 cm-diameter gelled Ag/AgCl electrode were placed on the forearm to record EMG simultaneously. (**B**) Raw signal recorded from electrodes during pinch grip (left) and during motion only (right). In the motion only condition, small deflections are seen during the up-down motions of the arm. (**C**) The same data shown in (B), after using a standard EMG bandpass filter from 85-300 Hz.

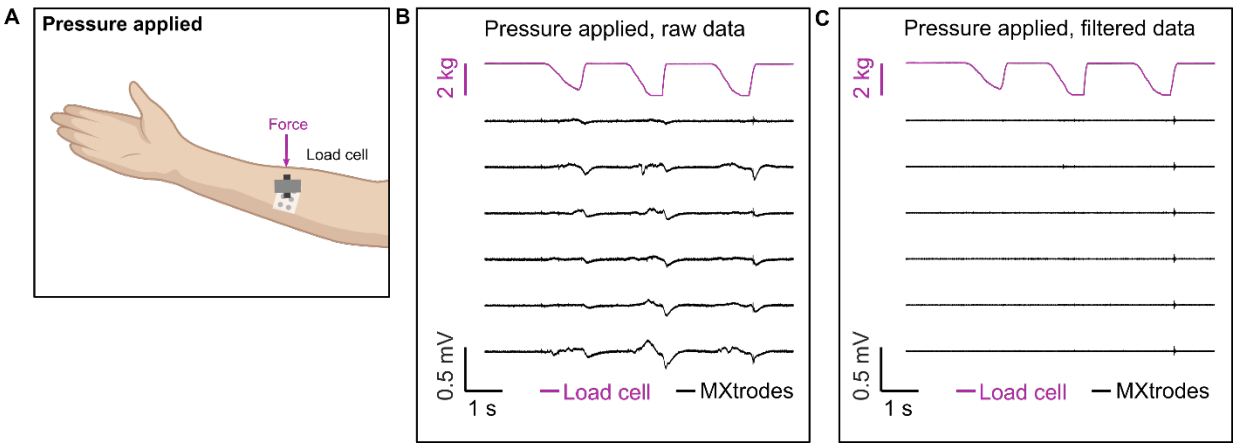

Fig. S13. Pressure-induced artifacts evaluation. (**A**) Schematic depicting the testing setup: a load cell was used to apply pressure onto 3 mm-diameter planar MXtrodes placed on the forearm to mimic pressures that might be experienced by EMG electrodes in a limb prosthetic socket. (**B**) Raw data recorded on MXtrodes in response to applied pressures, up to 2 kg. (**C**) The same data shown in (B) after using a standard EMG bandpass filter from 85-300 Hz.

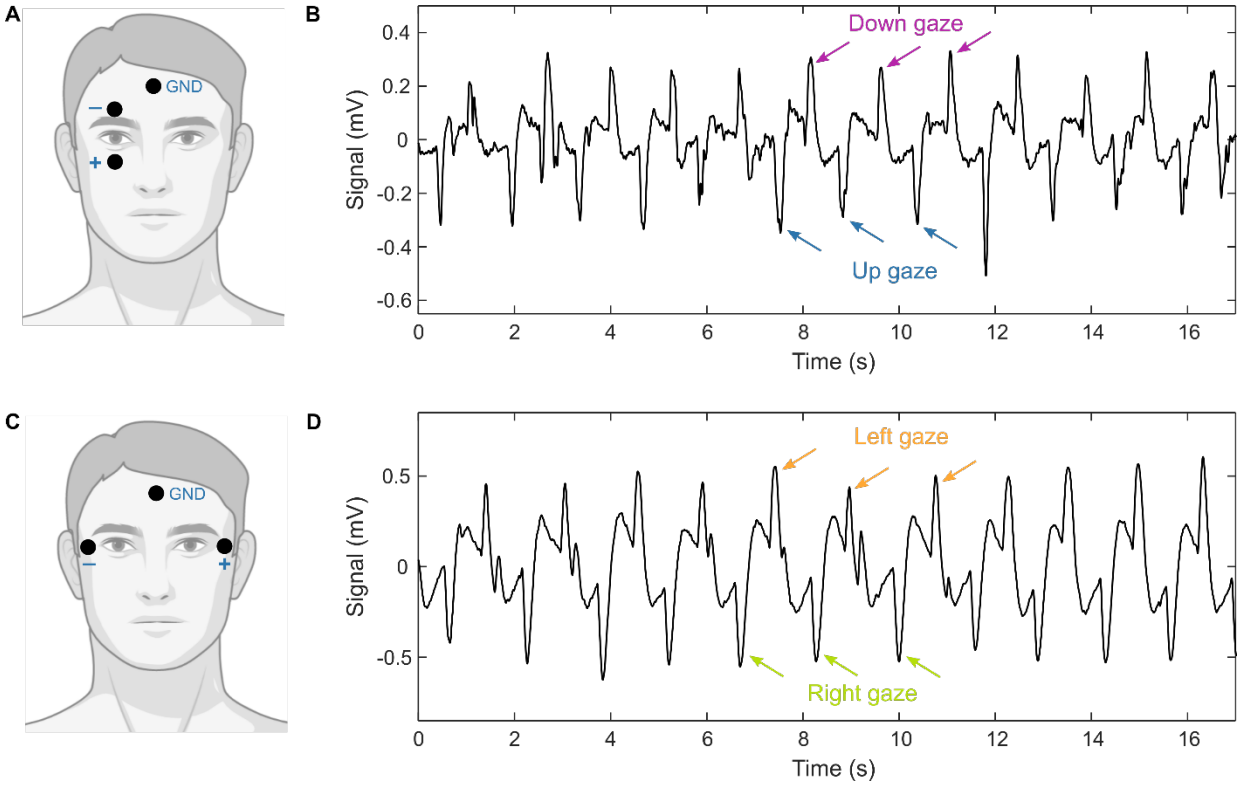

Fig. S14. Electrooculography with MXtrodes. (**A**) Schematic of EOG recording for monitoring up-down eye movements. (**B**) EOG data recorded on MXtrodes, showing distinct up and down eye movements. (**C**) Schematic of EOG recording for monitoring left-right eye movements. (**D**) EOG data recorded on MXtrodes, showing distinct left and right eye movements.

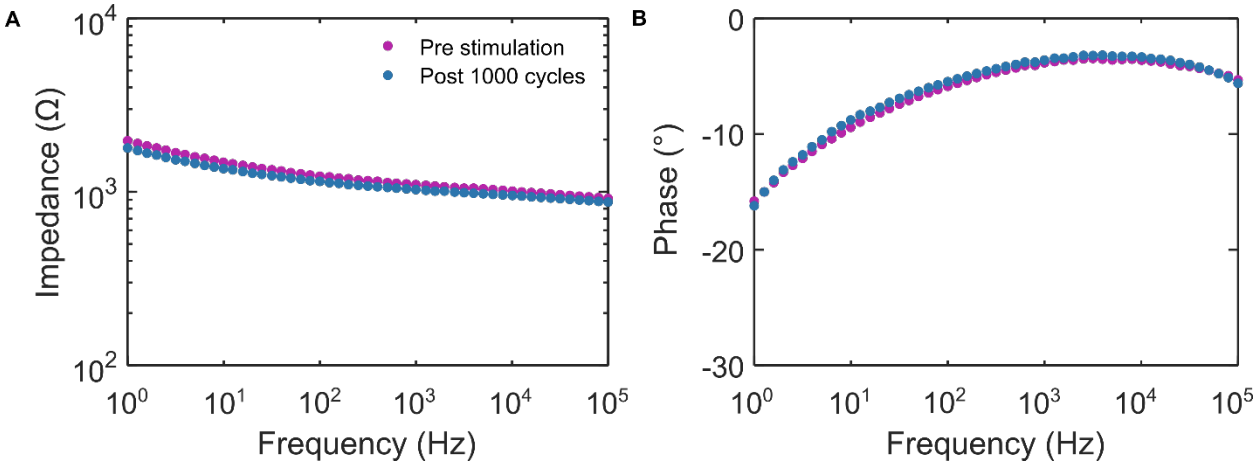

Fig. S15. Stability of MXtrodes to stimulation cycles. (**A**) Impedance magnitude and (**B**) phase for 500 µm-diameter MXtrodes in PBS before and after 1000 stimulation cycles of charge-balanced, cathodic-first pulses of 1.2 mA and 300 µs half-phase period.

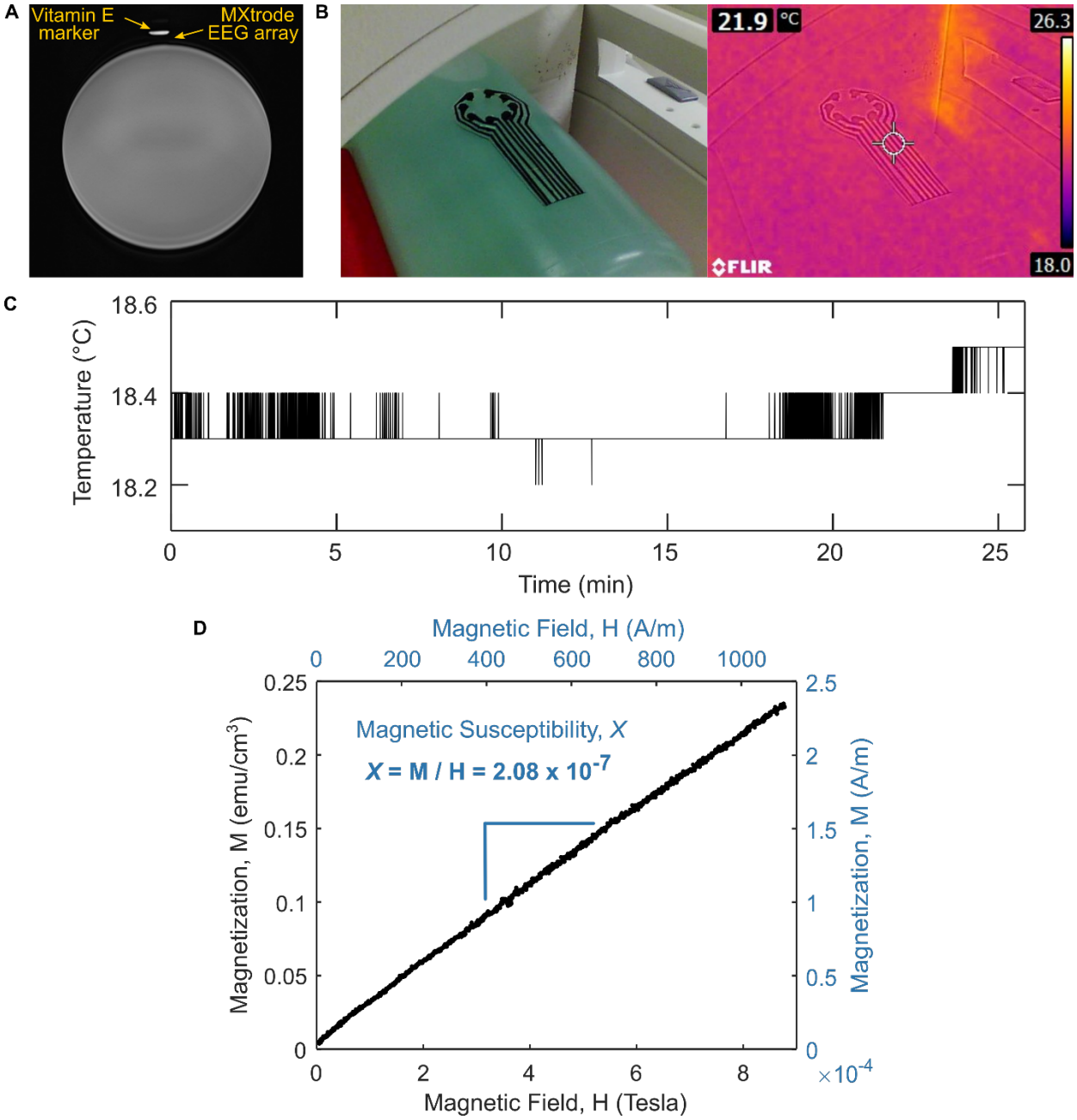

Fig. S16. 3T MRI compatibility and magnetic susceptibility of MXene. (**A)** MXtrode 3D mini-pillar EEG array, imaged on phantom in a 3T clinical MRI with a T2 weighted sequence. The array was placed atop the phantom and a Vitamin E marker was placed on top of the MXtrode array. (**B**) Photograph (left) and thermal infrared image (right) of MXtrode EEG array on the phantom captured immediately after a 10 min MRI sequence, showing no sign of heating. (**C**) Temperature of MXtrode mini-pillar electrode monitored continuously during a battery of scan sequences with a fiber optic sensor with 0.1 °C resolution. Temperature rose by 0.2 °C throughout the course of the scans. (**D**) Magnetic susceptibility of Ti_3C_2 MXene measured at body temperature (i.e., 310 K) for applied magnetic field up to 9T. For calculation of the magnetic susceptibility value, *X*, magnetization and field strength were both converted to units of A/m such that *X* is unitless.

Table S1. Electrochemical properties of MXtrode planar electrodes of varying diameters, 2 mm-diameter Pt electrodes, and literature values for other electrode materials. Scaling trends for each property are also shown in the top row. For each of the electrodes evaluated in this work N=10 for 1 kHz |Z|, and N=5 for CSC_C and CIC_C.

Material	Geometric Surface Area (mm^2)	1 kHz |Z| in PBS (Ω) ↑ elec size = ↓ |Z|	Potential Limits vs. Ag/AgCl (V)	CSC_C ($mC\ cm^{-2}$) ↑ elec size = ↓ CSC	CIC_C ($mC\ cm^{-2}$) ↑ elec size = ↓ CIC	Source
MXene	7.069	205.6 ± 11.1	-1.7 – 0.6	157.9 ± 19.6	0.53 ± 0.08	This work
	3.142	369.2 ± 40.2	-1.7 – 0.6	306.3 ± 35.2	0.67 ± 0.03	This work
	0.7854	430.2 ± 86.1	-1.7 – 0.6	607.8 ± 90.2	1.02 ± 0.07	This work
	0.1963	729.2 ± 71.2	-1.7 – 0.6	1495.3 ± 60.5	2.01 ± 0.46	This work
Pt	3.142	301.7 ± 77.6	-0.6 – 0.8	4.4 ± 0.7	0.05 ± 0.001	This work
Pt	3.142	1910 [a]	-0.6 – 0.8	3.6 [a]	0.17 [a]	*(61,92)*
Au	3.142	470 [a]	-0.9 – 0.6	0.3 [a]	0.21 [a]	*(61,92)*
PEDOT:PSS on Pt	3.142	1690 [a]	-0.9 – 0.6	2.3 [a]	0.18 [a]	*(61,92)*
PEDOT:PSS on Au	3.142	430 [a]	-0.9 – 0.6	1.0 [a]	0.86 [a]	*(61,92)*
Pt	0.1963	7790 [a]	-0.6 – 0.8	5.1 [a]	0.50 [a]	*(61,92)*
Au	0.1963	4430 [a]	-0.9 – 0.6	0.3 [a]	0.21 [a]	*(61,92)*
PEDOT:PSS on Pt	0.1963	2110 [a]	-0.9 – 0.6	3.7 [a]	0.66 [a]	*(61,92)*
PEDOT:PSS on Au	0.1963	990 [a]	-0.9 – 0.6	1.5 [a]	1.35 [a]	*(61,92)*
laser-roughened Pt	0.7854	760 [a]	-0.6 – 0.8	2.1 ± 0.1	0.026 [a]	*(57)*
PEDOT/CNT coating on Pt	0.0314	2100 [a]	-0.6 – 0.7	70	2.5 ± 0.1 [a]	*(93)*
Porous graphene (doped)	0.09	519	-1.3 – 0.8	50	3.1	*(94)*
CNT fiber	0.00145	11.2 ± 7.6 $x10^3$	-1.5 – 1.5	372 ± 56 [b]	6.52	*(95)*
TiN	0.004	11.5 $x10^3$ [a]	-0.9 – 0.9	2.47	0.55	(96)
IrOx	0.004	7.1 $x10^3$ [a]	-0.6 – 0.8	11	4	(96)
PtIr	5.985	125	-0.7 – 0.7	5.0	–	*(97)*

[a] Represents values extracted from plots from the respective references.

[b] CSC calculated from CV in Pt window, -0.6 to 0.8 V at 100 mV/s.

Table S2. CSC_C values for planar MXtrodes of varying diameters and the comparison Pt electrode. CV scans were performed at 50 mV/s for each electrode in both its water window and the intersection of the MXene and Pt water windows. For each measurement, N=5 electrodes evaluated.

Material	Electrode diameter	CSC_C (mC cm^{-2}) MXene window: -1.7 – 0.6 V	CSC_C (mC cm^{-2}) Intersection: -0.6 – 0.6 V	CSC_C (mC cm^{-2}) Pt window: -0.6 – 0.8 V
MXene	3 mm	157.9 ± 19.6	80.9 ± 8.9	N/A
	2 mm	306.3 ± 35.2	118.6 ± 10.1	N/A
	1 mm	607.8 ± 90.2	188.5 ± 28.4	N/A
	500 µm	1495.3 ± 60.5	288.7 ± 1.7	N/A
Pt	2 mm	N/A	4.0 ± 1.2	4.4 ± 0.7

1. R. J. Barry, A. R. Clarke, S. J. Johnstone, C. A. Magee, J. A. Rushby, EEG differences between eyes-closed and eyes-open resting conditions, *Clin. Neurophysiol.* **118**, 2765–2773 (2007).

2. M. A. Attiah, J. de Vries, A. G. Richardson, T. H. Lucas, A Rodent Model of Dynamic Facial Reanimation Using Functional Electrical Stimulation, *Front. Neurosci.* **11**, 193 (2017).

Movie legends

Movie S1. High-density dry EEG shows spatial patterns of alpha activation. Alpha bandpower, calculated in 1 s windows with 0.5 s of overlap, mapped over the electrode locations. The outer ring of electrodes are the dry MXtrodes and the center electrode is the standard gelled Ag/AgCl electrode.

Movie S2. High-density 32-ch bifrontal EEG shows spatial patterns of alpha activation. Alpha bandpower, calculated in 1 s windows with 0.01 s displacement, mapped over the electrode locations, showing clear spatial variations in activation. The raw signal from the electrode highlighted in the yellow box is shown at the top. One electrode is omitted due to poor scalp contact.

Movie S3. Cortical stimulation with MXtrodes evokes whisker movement in rat. Microstimulation of motor cortex with MXtrodes at 1.4 mV evokes whisker movements in anesthetized rat.

Data file legend

Data file S1. Individual subject-level data for $n < 20$. (Separate Excel file)